

# Online effective backscattering estimation for ring laser gyro

Zhenfang Fan (樊振方), Hui Luo (罗晖)\*, Guangfeng Lu (卢广锋), and Shaomin Hu (胡绍民)

College of Optoelectronic Science and Engineering, National University of Defense Technology, Changsha 410073, China

\*Corresponding author: nudtfzj@126.com

Received August 22, 2011; accepted December 12, 2011; posted online February 24, 2012

Lock-in phenomenon in ring laser gyroscopes is directly related to effective backscattering, which includes both backscattering and nonuniform loss. Effective backscattering often differs in different states and can only be reflected in a working state via online estimation in the working state. Moreover, effective backscattering can result in the intensity modulation of beams in the opposite directions. The effective backscattering parameters can be obtained by measuring the weak modulations in the intensity signals under different rotation rates and by using the curve-fitting method. This letter demonstrates the online estimation of backscattering.

OCIS codes: 140.3370, 140.3430, 230.5160.

doi: 10.3788/COL201210.051404.

Ring laser gyroscopes are now widely used in inertial navigation systems<sup>[1]</sup>, and the performances of these systems are significantly affected by the precision of these gyroscopes. The main error source in ring laser gyroscopes is the lock-in effect. Thus, the lock-in threshold should be reduced to enhance the gyroscope's performance<sup>[2,3]</sup>.

The lock-in of ring laser gyroscopes is related to both backscattering and nonuniform loss<sup>[4-6]</sup>. Square ring laser gyroscopes have four mirrors, and each mirror has scattering toward all directions. The scattering toward the incident direction is called backscattering, which can also be generated by the aperture. Backscattering can cause mutual energy coupling between beams in opposite directions of the cavity and has been proven to result in the lock-in phenomenon<sup>[4]</sup>. Aronowitz introduced a new type of energy coupling called "nonuniform loss," which spatially varied over the cavity length<sup>[6]</sup>. He stated that the behavior of nonuniform loss was the same as that of backscattering<sup>[6]</sup>. Thus, mathematically, the effect of both backscattering and nonuniform loss can be generalized as "effective backscattering," whose parameters should be measured. This letter discusses effective backscattering, which includes both backscattering and nonuniform loss.

Some methods have been proposed to measure backscattering directly using a passive cavity. However, these methods cannot estimate the contribution of nonuniform loss<sup>[7-9]</sup> nor reflect backscattering in the working state. Real backscattering and lock-in threshold can only be reflected in online estimation. Thus, this letter performs online backscattering estimation, where the backscattering parameters are obtained by measuring the modulation of the light intensity signals at different angle rates and by using the curve-fitting method.

The structure of a ring laser gyroscope is shown in Fig. 1. The housing is constructed from a crystallized glass block, into which holes are drilled for the tubes and electrodes<sup>[10]</sup>. The mirrors are attached to the block using optical contacts. The big hole in the center is used to mount the dither wheel for the bias<sup>[11]</sup>. The whole body of the ring laser gyroscope is designed to be highly symmetric to ensure good performance.

The cavity has two beams, namely, the clockwise (CW) and counterclockwise (CCW) beams. Their electromagnetic fields are  $E_1 e^{i(w_1 t + \chi_1)}$  and  $E_2 e^{i(w_2 t + \chi_2)}$ , respectively, where  $E_n$  is the amplitude and  $w_n t + \chi_n$  is the instantaneous phase. The backscattering in the mirrors and aperture causes a part of the CW beam to travel into the CCW direction every trip around the cavity and vice versa. The complex backscattering coefficients are denoted as  $r_1 e^{i\varepsilon_1}$  and  $r_2 e^{i\varepsilon_2}$ , respectively, where  $r_n$  is the backscattering amplitude and  $\varepsilon_n$  is the additional phase angle. The backscattering effect is shown in Fig. 2, where  $\psi$  is the beat frequency of the gyroscope.

The active media are considered as thermally moving atoms that acquire nonlinear electric dipole moments under the action of the field according to the laws of quantum mechanics by Lamb<sup>[12]</sup>. Based on Lamb's semiclassical theory, Aronowitz developed the following self-consistent equation for ring laser gyroscopes<sup>[13]</sup>.

$$\begin{aligned} \frac{\langle L \rangle}{c} \dot{I}_1 &= (\alpha_1 - \beta_1 I_1 - \theta_{12} I_2) I_1 - 2r_2 \sqrt{I_1 \cdot I_2} \cos(\psi + \varepsilon_2), \\ \frac{\langle L \rangle}{c} \dot{I}_2 &= (\alpha_2 - \beta_2 I_2 - \theta_{21} I_1) I_2 - 2r_1 \sqrt{I_1 \cdot I_2} \cos(\psi - \varepsilon_1), \\ \dot{\psi} &= \Omega + \frac{c}{\langle L \rangle} \left[ r_2 \sqrt{\frac{I_2}{I_1}} \sin(\psi + \varepsilon_2) \right. \\ &\quad \left. + r_1 \sqrt{\frac{I_1}{I_2}} \sin(\psi - \varepsilon_1) \right], \end{aligned} \quad (1)$$

where  $\langle L \rangle$  is the path length of the loop,  $c$  is the velocity of light,  $c/\langle L \rangle$  is the longitudinal mode spacing, and  $I_1$  and  $I_2$  are the dimensionless intensities of the two beams. In the two amplitude equations above,  $\alpha$  represents the gain minus loss every loop,  $\beta$  is the self-saturation coefficient,  $\theta$  is the mutual saturation coefficient, and  $\Omega$  is the input angle rate. The mode pulling term is not written explicitly because it can only induce the constant scale factor correction<sup>[14]</sup>. Aronowitz<sup>[6]</sup> introduced a new type of coupling called nonuniform loss. Mathematically, nonuniform loss can be included in the backscattering term. Therefore, the basic form of Eq. (1) does not change.

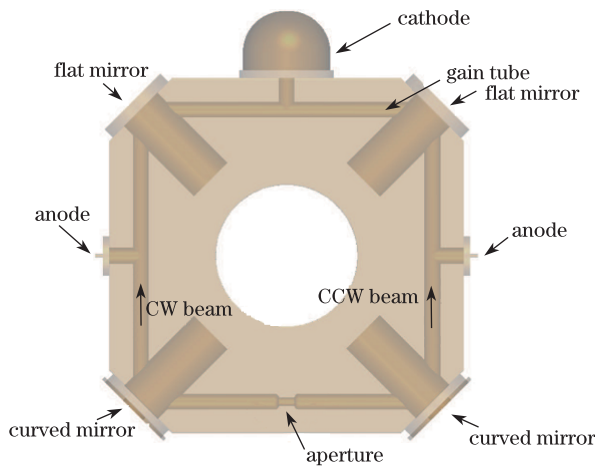


Fig. 1. Schematic of a ring laser gyroscope.

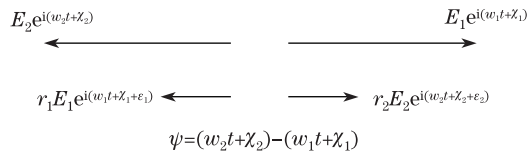


Fig. 2. Diagram of backscattering.

The structure of the ring laser gyroscope is designed to be symmetric such that the following are satisfied:

$$\begin{aligned} \alpha &= \alpha_1 = \alpha_2, \\ \beta &= \beta_1 = \beta_2, \\ \theta &= \theta_{12} = \theta_{21}, \\ r &= r_1 = r_2. \end{aligned} \quad (2)$$

After the following substitutions:

$$\begin{aligned} \varepsilon &= \varepsilon_1 + \varepsilon_2, \\ \phi &= \psi + \pi + \frac{1}{2}(\varepsilon_1 - \varepsilon_2), \\ I &= \frac{1}{2}(I_1 + I_2), \\ i &= \frac{1}{2}(I_1 - I_2), \end{aligned} \quad (3)$$

where  $I$  is the sum of the light intensities of the two beams and  $i$  is the difference between the light intensities, Eq. (1) can be written as<sup>[13]</sup>

$$\begin{aligned} \frac{\langle L \rangle}{c} \dot{I} &= [\alpha - (\beta + \theta) I] I + 2Ir \cos \phi \cos \varepsilon, \\ \frac{\langle L \rangle}{c} \dot{i} &= i(\alpha - 2\beta I) + 2Ir \cos \phi \cos \varepsilon, \\ \dot{\phi} &= \Omega - \frac{2c}{\langle L \rangle} r(\cos \varepsilon \sin \phi + \frac{i}{I} \sin \varepsilon \cos \phi). \end{aligned} \quad (4)$$

$I$  is believed to have steady and oscillation components  $I_0$  and  $\tilde{I}$ , respectively<sup>[15]</sup>:

$$I = I_0 + \tilde{I}. \quad (5)$$

Gao<sup>[15]</sup> analyzed Eq. (4) and obtained the following solution:

$$\begin{aligned} I_0 &= \frac{\alpha}{\beta + \theta}, \\ \tilde{I} &= I_0 \Omega_r \cos \varepsilon \frac{\Omega \sin(\Omega t) + \Omega_\alpha \cos(\Omega t)}{\Omega_\alpha^2 + \Omega^2}, \\ i &= I_0 \Omega_r \sin \varepsilon \frac{\Omega_i \sin(\Omega t) - \Omega \cos(\Omega t)}{\Omega_i^2 + \Omega^2}, \end{aligned} \quad (6)$$

where

$$\Omega_\alpha = \frac{c}{\langle L \rangle} \alpha, \quad \Omega_r = \frac{2cr}{\langle L \rangle}, \quad \Omega_i = \frac{\beta - \theta}{\beta + \theta} \cdot \Omega_\alpha. \quad (7)$$

The second and third equations of Eq. (6) can be written as

$$\begin{aligned} \frac{\tilde{I}}{I_0} &= \Omega_r \cos \varepsilon \frac{\sin(\Omega t + \eta_I)}{\sqrt{\Omega_\alpha^2 + \Omega^2}}, \\ \frac{i}{I_0} &= \Omega_r \sin \varepsilon \frac{\sin(\Omega t + \eta_i)}{\sqrt{\Omega_i^2 + \Omega^2}}, \end{aligned} \quad (8)$$

After the following substitutions:

$$\begin{aligned} I_A &= \frac{\Omega_r \cos \varepsilon}{\sqrt{\Omega_\alpha^2 + \Omega^2}}, \\ i_A &= \frac{\Omega_r \sin \varepsilon}{\sqrt{\Omega_i^2 + \Omega^2}}. \end{aligned} \quad (9)$$

Equation (8) can then be written as

$$\begin{aligned} \frac{\tilde{I}}{I_0} &= I_A \sin(\Omega t + \eta_I), \\ \frac{i}{I_0} &= i_A \sin(\Omega t + \eta_i). \end{aligned} \quad (10)$$

If the value of  $\Omega$  is changed, different values of  $I_A$  and  $i_A$  can be obtained. The parameters of Eq. (9) can be evaluated using the following curve-fitting method:

$$y = a/\sqrt{b^2 + x^2}, \quad (11)$$

where  $x$  is  $\Omega$  and  $y$  can be  $I_A$  or  $i_A$ . Nonlinear curve fitting must be used. This letter uses Newton's least square curve-fitting method.

A square ring laser gyroscope built in our laboratory was used to perform the experiment. The gyroscope was placed on a rotation table, and the wavelength of the laser was 632.8 nm. The longitudinal mode spacing  $c/\langle L \rangle$  was 1071 MHz. Signals  $\tilde{I}$  and  $i$  are very small and can therefore be easily covered by noise. Hence, the beat frequency signals must be used to demodulate  $\tilde{I}$  and  $i$ <sup>[16]</sup>. The rotation rate of the table was changed from 1 to 9 °/s, and both voltage representations of  $I_A$  and  $i_A$  for every rotation rate were recorded.

The experimental results are shown in Fig. 3. Data points with '+' denote the experimental data, and the continuous line is the curve after fitting.

After curve fitting, the parameters of Eq. (9) can be obtained as

$$\Omega_\alpha = 9.9088 \text{ }^\circ/\text{s}, \quad (12)$$

$$\Omega_i = 6.5344 \text{ }^\circ/\text{s}, \quad (13)$$

$$\Omega_r \cos \varepsilon = 0.0307 \text{ }^\circ/\text{s}, \quad (14)$$

$$\Omega_r \sin \varepsilon = 0.2215 \text{ }^\circ/\text{s}. \quad (15)$$

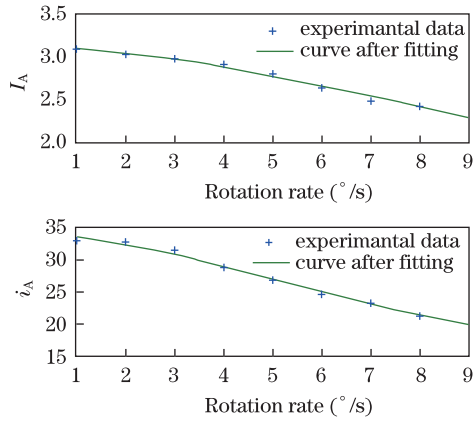


Fig. 3. Experimental results: Variations of (a)  $I_A$  and (b)  $i_A$  with rotation rate.

According to Eqs. (11) and (12), both  $I_A$  and  $i_A$  attenuate with the increase of rotation rate, but their curves are different. The shape of  $I_A$  is  $\frac{1}{\sqrt{\Omega_\alpha^2 + \Omega_i^2}}$ , whereas the shape of  $i_A$  is  $\frac{1}{\Omega_i^2 + \Omega_\alpha^2}$ . The curve of  $i_A$  is sharper than that of  $I_A$  because  $\Omega_\alpha > \Omega_i$ . From Eq. (7), the following can be obtained:

$$\frac{\Omega_i}{\Omega_\alpha} = \frac{\beta - \theta}{\beta + \theta}. \quad (16)$$

Moreover, the values in Eqs. (11) and (12) can be used to obtain

$$\frac{\beta - \theta}{\beta + \theta} = \frac{6.5344 \text{ }^\circ/\text{s}}{9.9088 \text{ }^\circ/\text{s}} = 0.66. \quad (17)$$

Equation (17) shows that the difference between  $\Omega_\alpha$  and  $\Omega_i$  is a result of the self- and mutual saturations between the two beams.

According to Eqs. (14) and (15),

$$\Omega_r = \sqrt{(\Omega_r \cos \varepsilon)^2 + (\Omega_r \sin \varepsilon)^2} = 0.2237 \text{ }^\circ/\text{s}. \quad (18)$$

The unit of  $\Omega_r$  in Eq. (18) is expressed in degrees per second ( $^\circ/\text{s}$ ). Thus, the scale factor must be applied to get the value of  $\Omega_r$  in hertz. The scale factor of the gyroscope is  $1930 \text{ Hz}/(^\circ/\text{s})$ . Therefore, the value of  $\Omega_r$  in hertz is

$$\Omega_r = 431.7 \text{ Hz}. \quad (19)$$

According to the second term in Eq. (7), the value of the backscattering magnitude  $r$  can be evaluated as

$$r = \frac{\Omega_r \langle L \rangle}{2c} = 6.3 \times 10^{-7}. \quad (20)$$

If Eq. (14) is divided by Eq. (15), then

$$\tan \varepsilon = \frac{\Omega_r \sin \varepsilon}{\Omega_r \cos \varepsilon} = \frac{0.2215 \text{ }^\circ/\text{s}}{0.0307 \text{ }^\circ/\text{s}} = 7.215. \quad (21)$$

The backscattering angle  $\varepsilon$  can be evaluated as

$$\varepsilon = \arctan 7.215 = 82.1^\circ. \quad (22)$$

In conclusion, we experimentally demonstrate the on-line estimation of backscattering by evaluating the modulations of the intensity signals at different input angle rates. The results are helpful in the assessment of ring laser gyroscopes. They can also serve as guide in the reduction of lock-in threshold and further enhancement of ring laser gyroscope performance.

This work was supported by the Program for New Century Excellent Talents in University 2010.

## References

1. M. Faucheux, D. Fayoux, and J. J. Roland, *J. Opt.* **19**, 101 (1988).
2. S.-W. Song, J.-C. Lee, S.-K. Hong, and D. Chwa, *J. Opt.* **12**, 115501 (2010).
3. Z. Fan, H. Luo, S. Hu, and G. Xiao, *Opt. Eng.* **50**, 034403 (2011).
4. F. Aronowitz and R. J. Collins, *Appl. Phys. Lett.* **9**, 55 (1966).
5. R. Spreeuw, R. C. Neelen, N. Van Druten, E. Eliel, and J. Woerdman, *Phys. Rev. A* **42**, 4315 (1990).
6. F. Aronowitz, *J. Appl. Phys.* **41**, 2453 (1970).
7. J. Wu and X. Long, *Laser & Infrared (in Chinese)* **29**, 347 (1999).
8. L. Cao, Q. Lin, and H. Wang, *Aviat. Prec. Manu. Technol. (in Chinese)* **29**, 8 (1993).
9. D. R. Jungwirth, "Ring laser cavity backscatter measurement" US Patent 5090812 (1992).
10. G. Xiao, X. Long, B. Zhang, and G. Li, *Chin. Opt. Lett.* **9**, 101201 (2011).
11. J. E. Killpatrick, "Laser angular rate sensor" US Patent 3373650 (1968).
12. W. E. Lamb, *Phys. Rev.* **134**, 1429 (1964).
13. F. Aronowitz, *Phys. Rev.* **139**, 635 (1965).
14. F. Aronowitz and J. E. Killpatrick, *IEEE J. Quantum Electron.* **10**, 201 (1974).
15. B. L. Gao, *J. NUDT (in Chinese)* **S**, 1 (1979).
16. Z. F. Fan, H. Luo, G. F. Lu, and X. Cheng, *Proc. SPIE* **8192**, 81922E (2011).